PCP
PLANT & CELL PHYSIOLOGY

Rapid Paper

Phosphorylation of RNA Polymerase II by CDKC;2 Maintains the Arabidopsis Circadian Clock Period

Takahiro N. Uehara[1,†], Takashi Nonoyama[2,†], Kyomi Taki[2,†], Keiko Kuwata[3], Ayato Sato[3], Kazuhiro J. Fujimoto[1,3], Tsuyoshi Hirota[3], Hiromi Matsuo[4], Akari E. Maeda[2], Azusa Ono[2], Tomoaki T. Takahara[5], Hiroki Tsutsui[2], Takamasa Suzuki[6], Takeshi Yanai[1,3], Steve A. Kay[7], Kenichiro Itami[1,3,8], Toshinori Kinoshita[2,3], Junichiro Yamaguchi[5,*] and Norihito Nakamichi[4,*]

[1]Department of Chemistry, Graduate School of Science, Nagoya University, Furo-cho, Chikusa, Nagoya, 464-8602 Japan
[2]Division of Biological Science, Graduate School of Science, Nagoya University, Furo-cho, Chikusa, Nagoya, 464-8602 Japan
[3]Institute of Transformative Bio-Molecules (WPI-ITbM), Nagoya University, Furo-cho, Chikusa, Nagoya, 464-8601 Japan
[4]Graduate School of Bioagricultural Sciences, Nagoya University, Furo-cho, Chikusa, Nagoya, 464-8601 Japan
[5]Department of Applied Chemistry, Waseda University, 513 Wasedatsurumakicho, Shinjuku, Tokyo, 162-0041 Japan
[6]College of Bioscience and Biotechnology, Chubu University, 1200 Matsumoto-cho, Kasugai, 487-8501 Japan
[7]Keck School of Medicine, University of Southern California, 1975 Zonal Avenue, Los Angeles, CA 90033, USA
[8]JST ERATO, Itami Molecular Nanocarbon Project, Nagoya University, Furo-cho, Chikusa, Nagoya, 464-8602 Japan
[†]These authors contributed equally to this work.

The DDBJ Sequence Read Archive with accession number DRA009508.

*Corresponding authors: Norihito Nakamichi, E-mail, nnakamichi@itbm.nagoya-u.ac.jp; Junichiro Yamaguchi, E-mail, junyamaguchi@waseda.jp

(Received 27 December 2021; Accepted 25 January 2022)

The circadian clock is an internal timekeeping system that governs about 24 h biological rhythms of a broad range of developmental and metabolic activities. The clocks in eukaryotes are thought to rely on lineage-specific transcriptional–translational feedback loops. However, the mechanisms underlying the basic transcriptional regulation events for clock function have not yet been fully explored. Here, through a combination of chemical biology and genetic approaches, we demonstrate that phosphorylation of RNA polymerase II by CYCLIN DEPENDENT KINASE C; 2 (CDKC;2) is required for maintaining the circadian period in Arabidopsis. Chemical screening identified BML-259, the inhibitor of mammalian CDK2/CDK5, as a compound lengthening the circadian period of Arabidopsis. Short-term BML-259 treatment resulted in decreased expression of most clock-associated genes. Development of a chemical probe followed by affinity proteomics revealed that BML-259 binds to CDKC;2. Loss-of-function mutations of *cdkc;2* caused a long period phenotype. In vitro experiments demonstrated that the CDKC;2 immunocomplex phosphorylates the C-terminal domain of RNA polymerase II, and BML-259 inhibits this phosphorylation. Collectively, this study suggests that transcriptional activity maintained by CDKC;2 is required for proper period length, which is an essential feature of the circadian clock in Arabidopsis.

Keywords: *Arabidopsis thaliana* (Arabidopsis) • CDKC;2 • Chemical screening • Circadian clock • Pol II phosphorylation

Editor-in-Chief's Choice

Introduction

The circadian clock is an internal timekeeping system that governs a broad range of biological activities, by which the organisms are able to predictively respond to diurnal changes from environment. The circadian clock also gives competitive advantages to organisms such as cyanobacteria and plants grown under day–night cycles (Woelfle et al. 2004, Dodd et al. 2005, Yerushalmi et al. 2011). The circadian clock has three fundamental characteristics: self-sustaining oscillation under constant conditions, temperature compensation of period length and entrainment by environmental time cues such as light input. The pacemaker of the circadian clock in cyanobacteria is the KaiC phosphorylation cycle, whereas the clocks in eukaryotes depend on the common architecture of interlocked transcription–translation feedback loops (TTFLs) (Nakajima et al. 2005, Doherty and Kay 2010). The TTFL involves the general transcription and translation reactions; however, pharmacological inhibition of the general transcription and translation results in no or only slight effects on circadian period length in animals or the algae (Karakashian and Hastings 1962, Dibner et al. 2009, Nakajima et al. 2015).

The TTFL has been proposed as a core clock mechanism in the flowering plant *Arabidopsis thaliana* (Arabidopsis) (Nohales and Kay 2016, Shalit-Kaneh et al. 2018). Transcription factors CIRCADIAN CLOCK-ASSOCIATED 1 (CCA1), LATE ELONGATED HYPOCOTYL (LHY); the PSEUDO-RESPONSE REGULATOR (PRR) family, including TIMING OF CAB EXPRESSION1 (TOC1); Evening Complex (EC) constituted with EARLY

Plant Cell Physiol. 63(4): 450–462 (2022) doi:https://doi.org/10.1093/pcp/pcac011, Advance Access publication on 27 January 2022, available online at https://academic.oup.com/pcp

FLOWERING 3 (ELF3), ELF4, and LUXARRHYTHMO (LUX); the LIGHT-INDUCIBULE AND CLOCK-REGULATED (LNK) family; and the REVELLE (RVE) family are expressed during specific time periods throughout the day, forming a TTFL (Nohales and Kay 2016). The molecular mechanisms that control clock transcriptional regulation have more recently come to light. The three PRRs, CCA1 and LHY all repress target genes by associating with histone deacetylases (Wang et al. 2013, Hung et al. 2018). EC modulates chromatin domains to repress target gene loci (Tong et al. 2020). The LNK1–RVE8 complex physically associates with components of general transcription machinery such as RNA polymerase II (Pol II) to activate target genes (Xie et al. 2014, Ma et al. 2018). Mutants impaired in the splicing of clock genes have an abnormal long-period phenotype, suggesting that post-transcriptional events are also crucial for normal clock functioning (Sanchez et al. 2010, Jones et al. 2012). Although transcriptional and post-transcriptional events have been considered essential elements for plant clock regulation, the proteins involved in this process are largely unknown except for the examples given above, likely due to the technical problems associated with genetic redundancy or essentiality.

Chemical genetics approaches are emerging as methodologies that can be used to reveal molecular mechanisms underlying biological systems in plants by overcoming redundant gene functions or other technical limitations (Dejonghe and Russinova 2017). One advantage of chemical genetics is that utilizing small molecules gives useful phenotypic information by directly targeting redundant or essential proteins. Screening small molecules for specific biological activities followed by a detailed examination of action mechanisms eventually provides a much deeper understanding of biological systems than other approaches that are limited by genetic redundancy or lethality by genetic mutation (Zhang et al. 2016, Uehara et al. 2019).

Here, we report that chemical treatment with the small molecule BML-259, *N*-(5-isopropyl-2-thiazolyl) phenylacetamide (**Fig. 1A**), a known inhibitor of cyclin-dependent kinase 5 (CDK5) and CDK2 in mammals (Helal et al. 2004), lengthens the circadian period in Arabidopsis. An affinity-proteomics approach using a molecular probe indicated that CYCLIN DEPENDENT KINASE C;2 (CDKC;2) and CDKC;1 are candidate targets of BML-259. Circadian periods were longer in *cdkc;2* mutants compared to the wild-type. BML-259 attenuated Ser 5 phosphorylation of the Pol II C-terminal domain (CTD) repeat, which is phosphorylated by the CDKC;2 immunocomplex in vitro. This study connects phosphorylation of general transcription machinery with maintenance of proper circadian period length in Arabidopsis.

Results and Discussion

BML-259 lengthens the Arabidopsis circadian clock period

Small molecules that change the Arabidopsis circadian period were screened using a transgenic line expressing luciferase under the control of the *CCA1* promoter (*CCA1:LUC*), which has peak expression during the early morning (Uehara et al. 2019). BML-259 was identified as a period lengthening molecule from a mammal kinase inhibitor library (**Fig. 1A–C**). BML-259 is an inhibitor of cyclin-dependent kinase 5 (CDK5) and CDK2 in mammals (Helal et al. 2004). Mammal CDK2 drives cell cycle progression, and CDK5 regulates neuronal development (Chu et al. 2021). Continuous treatment with BML-259 also lengthened the circadian period of evening-peaked *TOC1:LUC* reporter in a dose-dependent manner (**Fig. 1D, E**). BML-259 treatment at 50 μM resulted in lengthening for both *CCA1:LUC* and *TOC1:LUC* reporters for at least 8 h (**Fig. 1C, E**). Luminescence of both reporters decreased with treatment of BML-259 at 50 μM (**Fig. 1B, D**). At 500 μM, BML-259 caused bleaching of cotyledons and inhibition of true leaf emergence, indicating toxic activity at higher doses (**Supplementary Fig. S1**).

To understand the action mechanism of BML-259 for clock control, we observed whether the expression of specific clock-associated genes is altered by short-term treatment of BML-259. Seedlings were treated with BML-259 for 3 hours, RNA from whole seedlings was extracted and RNAseq analysis was performed (Dataset S1A and **Fig. 1F, G**). Even if the stringent statistical values were applied, treatment with 27 μM BML-259 resulted in 181 up-regulated and 4,554 down-regulated genes compared with solvent DMSO treatment as control experiment, suggesting BML-259 has a large impact on the transcriptome at the concentration that lengthened period (**Fig. 1F**, false discovery rate (FDR) $q < 10^{-10}$ and 10-fold change, Dataset S1B and C). Enriched Gene Ontology (eGO) analysis showed that 'response to hypoxia', 'response to chemical treatment' and 'response to drug treatment' were enriched among the 181 up-regulated genes, suggesting that BML-259 treatment forced Arabidopsis to induce general stress responses to chemical compounds (**Supplementary Fig. S2**). A wide range of biological processes that were called as eGO terms among the 4,554 down-regulated genes (e.g. 'nucleic acid metabolic process', 'regulation of gene expression', 'macromolecule modification', **Supplementary Fig. S2**). There were no eGO terms specifically related to circadian clock among the 4,554 genes. We found that, compared to rhythmic genes, non-rhythmic genes were slightly but statistically down-regulated by BML-259 (**Fig. 1H**). These data suggest that BML-259 down-regulates many genes from a wide array of cellular functions.

When we examined the clock gene expression upon BML-259 treatment, we found that the amount of clock-associated gene transcription, except for *PRR5*, *PRR3*, *NOX* and *LNK2*, was reduced by 27 μM BML-259 treatment (**Fig. 1F, G**). For example, expression of *ELF3*, *SPLICEOSOMAL TIMEKEEPER LOCUS1* (*STIPL1*), *TIME FOR COFFEE* (*TIC*), *LIGHT-REGULATED WD 2* (*LWD2*) and *GIGANTEA* (*GI*) were strongly down-regulated by BML-259 (also found in 4,554 down-regulated genes in Dataset S1C, blue dots in **Fig. 1F**). A dawn phase-expressed gene *CCA1*, morning phase-expressed genes *LNK1* and *RVE8*, and an evening phase-expressed *TOC1*, and even in constantly

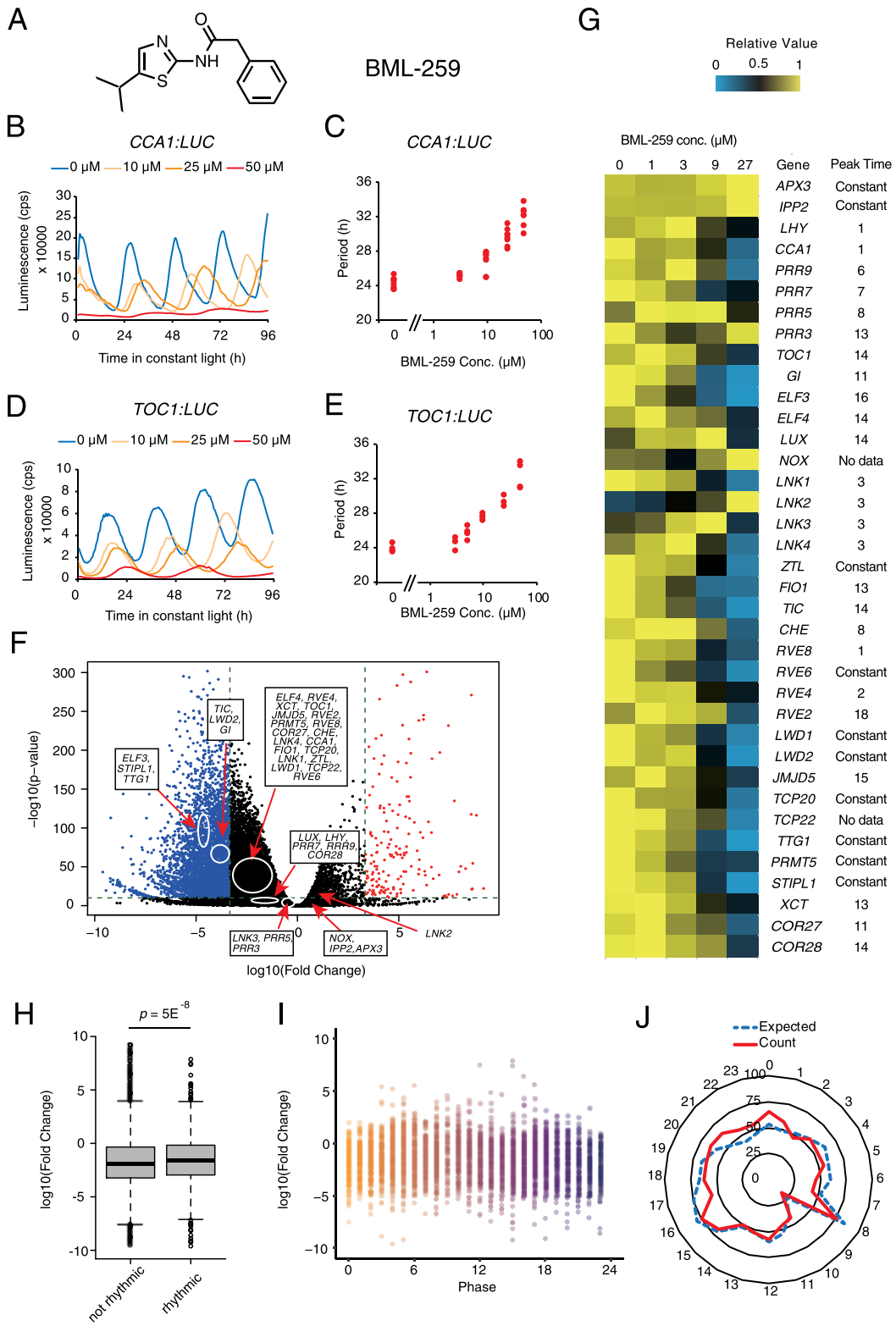

Fig. 1 The small molecule BML-259 lengthens circadian period in Arabidopsis. (A) Chemical structure of BML-259. Representative traces of circadian luciferase reporter *CCA1:LUC* (B) and *TOC1:LUC* (D) activity in Arabidopsis with BML-259 treatment. Increases in period length relative to untreated (0 μM) control indicate a dose response (C) and (E) ($n = 7$ or 8 for each concentration for (C), $n = 3$ or 4 for (E)). (F) Volcano plot of transcriptome change by 27 μM BML-259. Blue and red dots are down-regulated and up-regulated genes by BML-259 (FDR $q < 10^{-10}$ and 10-fold change). (G) Circadian clock genes expression with 0–27 μM BML-259 treatment. Means from three biological replicates were used to make the heatmap. Peak time of gene expression was surveyed using the Phaser webtool. RNAseq data were normalized by counts per million (CPM) as detailed in Dataset S1. Maximal value for each gene was set to a relative value of '1'. (H) and (I) Expression change of non-cyclic and cyclic genes by 27 μM BML-259. (J) Circadian phases of down-regulated genes by 27 μM BML-259. The radial axis showed circadian time.

expressed *ZEITLUPE* (*ZTL*) were decreased by BML-259 treatment (FDR $q < 10^{-10}$ and 2-fold decrease, **Fig. 1F, G**). BML-259-dependent down-regulation was not limited to any specific set of time-of-day genes (**Fig. 1I, J**). Collectively, BML-259 can modulate the expression of most clock-associated genes.

CDKC;2 is a possible target of BML-259

Given that period lengthening molecules PHA767491 and 3, 4-dibromo-7-azaindole inhibit Arabidopsis CKL proteins (Ono et al. 2019, Saito et al. 2019, Uehara et al. 2019), we tested whether the BML-259 targets CKL family for period lengthening. PHA767491 at 10 μM, a which was biologically active concentration (Uehara et al. 2019), strongly inhibited CKL4 kinase activity, whereas the biologically active concentration of BML-259 did not (**Supplementary Fig. S3**), suggesting that BML-259 lengthens the circadian period via CKL-independent pathways.

In order to identify the direct molecular targets of BML-259, an affinity-based proteomic approach was used, first by performing a structure–activity relationship study using synthetic BML-259 derivatives to reveal which positions of BML-259 could be linker-conjugated (**Fig. 2A**). BML-259 derivatives were synthesized as described in Supplementary note 1. We firstly tested whether the C5 position of the thiazole ring of BML-259 is suitable for linker-conjugation. The circadian period was about 50 h after treatment with 100 μM of BML-259 (**Fig. 2A**). Treatment with a non-substituted compound (**1b**) did not result in period lengthening (**Fig. 2A**), but cyclobutyl- (**1a**), bromo- (**1c**) or methyl- (**1d**) substituted molecules did lengthen the period. These results indicate that a substituent at the C5 position of the thiazole is crucial for period-lengthening activity, excluding this position for consideration as a site for linker-conjugation. Two derivatives with a methoxy group at the C4 position of the phenyl group (**1e**) and an *N*-methylation at the amide N-H bond (**1f**) were also tested for period-lengthening activity. Derivative **1e** lengthened the period significantly, whereas **1f** did not. This result suggested that the phenyl group at the *para* position, but not at the amide position, is suitable for linker-conjugation. Therefore, derivative **2**, which has an ethoxy linker at the *para* position of the phenyl group, was made to be directly conjugated to agarose beads. Compound **2** had period-lengthening activity (**Fig. 2B**, **Supplementary Fig. S4**), confirming that the molecule is a suitable molecule for target identification of BML-259.

BML-259 beads were generated by covalently conjugating compound **2** to agarose beads. BML-259-conjugated beads were incubated with Arabidopsis seedling lysates with or without excess amounts of BML-259 as a competitor to inhibit interactions between compound **2** beads and target proteins. Two independent experiments showed that CYCLIN DEPENDENT KINASE C;2 (CDKC;2), CDKC;1 and CRYPTOCHROME1 (CRY1) were BML-259-beads-bound proteins, but binding decreased to almost zero with excess BML-259 (50 μM) (**Fig. 2C**). 50 μM BML-259 is a concentration that gives about 4–8 h period

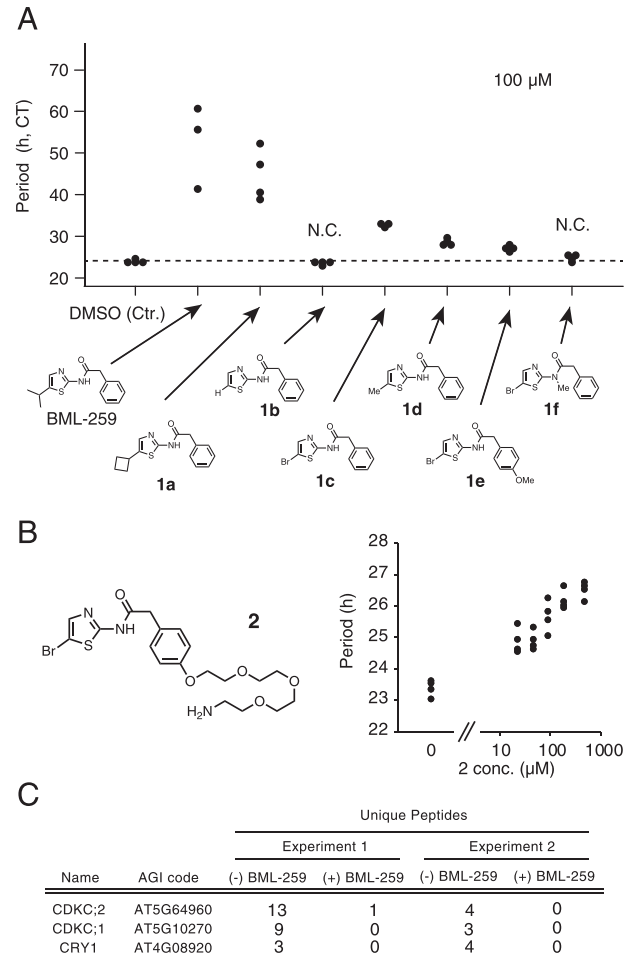

C

		Unique Peptides			
		Experiment 1		Experiment 2	
Name	AGI code	(-) BML-259	(+) BML-259	(-) BML-259	(+) BML-259
CDKC;2	AT5G64960	13	1	4	0
CDKC;1	AT5G10270	9	0	3	0
CRY1	AT4G08920	3	0	4	0

Fig. 2 CDKC;2 is bound by BML-259 beads. (A) Structure–activity relationship study of BML-259 for period lengthning. Clock period change was determined as compared to a DMSO treatment control with each concentration at 100 μM, $n = 3$ or 4. Means were compared by Student's t-test with the DMSO control (N.C. indicates no change). (B) Period lengthening activity of compound 2. (C) Proteins bound by BML-259 beads were analyzed by LC–MS/MS. BML-259 was added as the competitor.

lengthening (**Fig. 1**). These results suggested that CDKCs and CRY1 are target candidates of BML-259.

cdkc;2-2 mutants have a long circadian period phenotype

Arabidopsis CRY1 is a blue light receptor involved in the light input pathway that resets the circadian clock. The period length of *cry1* mutants is longer than that of wild-type under certain light conditions (Somers et al. 1998), implying that BML-259 inhibits CRY1. To test this hypothesis, we examined in vivo CRY1 activity following BML-259 treatment. Hypocotyl length control under blue-light is a robust assay for analyzing CRY1 activity (Lin 2002), in which hypocotyls of *cry1* mutants are more elongated under blue-light conditions than wild-type. BML-259 treatment resulted in shorter hypocotyls than DMSO treatment under

blue light conditions, indicating that BML-259 does not inhibit CRY1 function (**Supplementary Fig. S5**). As further evidence to rule out CRY1 as a target for BML-259 for period lengthening, 3-bromo-7-nitroindazole, a small-molecule inhibitor of CRY1 (Ong et al. 2017), did not extend period length under our experimental conditions (**Supplementary Fig. S5**). CRY1 is therefore an unlikely target of BML-259 for period lengthening.

CDKC;1 and CDKC;2 are kinases that phosphorylate the CTD of RNA polymerase II (Pol II) (Cui et al. 2007). It has been proposed that the CDKC family proteins are homologues of mammalian CDK9 based on their sequence similarities (Cui et al. 2007, Wang et al. 2014). Our phylogenetic analysis using kinase domains suggested that two CDKCs are also similar to mammalian CDK12 and CDK13 (**Supplementary Fig. S6**). Mammalian CDK9, CDK12 and CDK13 phosphorylate the Pol II CTD at different amino acid residues. CDK9 phosphorylates Ser 5, whereas CDK12 preferentially phosphorylates Ser 5, and can also phosphorylate Ser 2 (Bosken et al. 2014). *CDKC;2* loss-of-function mutants typically have attenuated transcription of genes involved in diverse functions such as vernalization and virus infection (Cui et al. 2007, Wang et al. 2014).

To examine the possibility of involvement of *CDKC* genes in circadian clock regulation, we firstly tested the circadian period length of a T-DNA insertion loss-of-function mutant line for *CDKC;2* (*cdkc;2-2 CCA1:LUC*) (**Fig. 3A**).

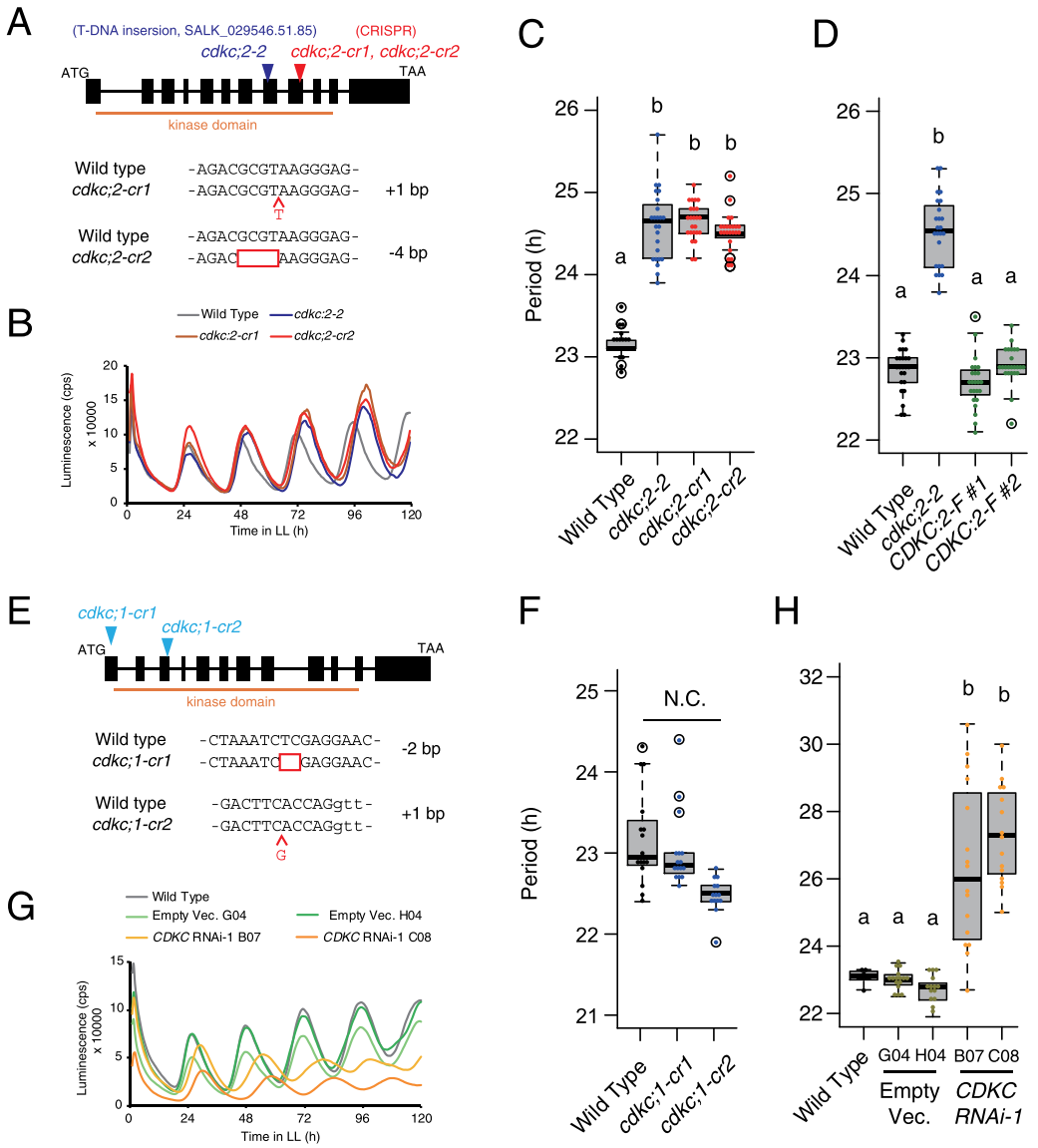

Fig. 3 *CDKC;2* is required for proper period length. (A) Map of mutation points of the *CDKC;2* gene. (B) Representative traces of a single replicate of *CCA1:LUC* reporter in three *cdkc;2* mutants. *CCA1:LUC* circadian period length of the *cdkc;2* mutants (C), and *CDKC;2pro:CDKC;2-FLAG/cdkc;2-2* lines (*CDKC;2-F* #1 and #2) ($n = 23$ or 24) (D). (E) Mutation points of the *CDKC;1*. (F) Period length of *cdkc;1* mutants ($n = 14 \sim 16$). (G) Traces of a single replicate of the reporter in *CDKC* RNAi-1 lines. (H) Period of the *CDKC* RNAi-1 lines ($n = 24$). Letters above the bars indicate statistical differences determined by the Tukey–Kramer test ($P < 0.01$).

The phenotype of *cdkc;2-2* showed a longer period than wild-type (**Fig. 3B, C**, **Supplementary Fig. S7**). To confirm the relationship between the *cdkc;2* mutation and long period, we made additional *cdkc;2* mutants by CRISPR-Cas9 (Clustered Regularly Interspaced Short Palindromic Repeats/CRISPR-associated 9) mediated genome editing in the *CCA1:LUC* reporter line (**Fig. 3B, C**, **Supplementary Fig. S7**). The resulting two mutants *cdkc;2-cr1* and *cdkc;2-cr2* had longer periods than wild-type. To further confirm that *CDKC;2* is required for maintaining proper period length, we introduced a genomic fragment of *CDKC;2* fused to the FLAG protein tag into *cdkc;2-2* (*CDKC;2pro:CDKC;2-FLAG cdkc;2-2 CCA1:LUC*, namely *CDKC;2-F*). Introduction of *CDKC;2-FLAG* resulted in complementation of the long period phenotype of *cdkc;2-2*, confirming that *CDKC;2* is required for maintaining circadian period length (**Fig. 3D**, **Supplementary Fig. S7**).

Two independent *cdkc;1* mutants were created by CRISPR-Cas9-mediated genome editing (*cdkc;1-cr1* and *cdkc;1-cr2*) using *CCA1:LUC* as the parental plants (**Fig. 3E**). Both of these lines are null for *CDKC;1* due to the generation of nonsense mutations, resulting in the disruption of the kinase domain. Neither *cdkc;1-cr1* nor *cdkc;1-cr2* had a long period phenotype (**Fig. 3F**, **Supplementary Fig. S7**). It would be useful to generate *cdkc;1 cdkc;2* double loss-of-function mutants to conclusively determine whether or not *CDKC;1* regulates circadian periodicity when *CDKC;2* is non-functional, but we were unable to obtain double loss-of-function mutants, likely due to the lethality by loss of the essential role of both of the redundant *CDKC* genes (**Supplementary Fig. S8**), as had previously been suggested (Cui et al. 2007). The *cdkc;2-2* (homozygous)/*cdkc;1-cr1* (heterozygous) plants showed growth retardation and were not viable after transfer to soil. Seed maturation of *cdkc;2-2* (heterozygous)/*cdkc;1-cr1* (homozygous) plants was 60–80%, whereas those of *cdkc;1-cr1* (homozygous) and *cdkc;2-2* (homozygous) were >95%, indicating that double mutants are lethal (**Supplementary Fig. S8**). To get around this problem, we simultaneously knocked down *CDKC;1* and *CDKC;2* with an RNA interference construct (*CDKC* RNAi-1). Seedlings in which the expression of both *CDKC;1* and *CDKC;2* was decreased by *CDKC* RNAi-1 had periods that were lengthened by 2–5 h compared to control seedlings (**Fig. 3G, H**, **Supplementary Figs. S7, S9**). A long period phenotype was also obtained by another RNA interference construct, *CDKC* RNAi-2 (**Supplementary Fig. S9**), suggesting that simultaneous knockdown of *CDKC;1* and *CDKC;2* results in longer circadian periods than does the *cdkc;2* mutation alone. Compared with wild-type, *cdkc;2* single mutants and the *CDKC;1 CDKC;2* RNAi lines were more sensitive to BML-259 (**Supplementary Fig. S10**). It is therefore likely that BML-259 inhibits CDKC function more efficiently in the *cdkc;2* mutants or *CDKC;1 CDKC;2* RNAi lines than in wild-type.

BML-259 inhibits kinase activity of the CDKC;2 immunocomplex

To investigate whether BML-259 directly affects CDKC;2 kinase activity, we examined the kinase activity of CDKC;2-FLAG purified from *CDKC;2-F*, plants. CDKC;2-FLAG protein was immunoprecipitated from plants with anti-FLAG antibody (**Supplementary Fig. S11**) and incubated with GST-CTD and ^{32}P-ATP. We observed a faint radioactive signal in the immunoprecipitated fraction from *cdkc;2-2* and strong radioactive signal from the SDS gel band of the predicted CDKC;2-F size from *CDKC;2-F* plants (**Supplementary Fig. S11**). Recombinant GST-CTD (~25-kDa band) was not phosphorylated if it was incubated with the anti-FLAG-immunoprecipitated fraction from *cdkc;2-2*. However, GST-CTD, but not GST alone, was phosphorylated by the immunoprecipitated fraction from CDKC;2-F (**Supplementary Fig. S11**). These results showed that the CDKC;2-FLAG immunocomplex phosphorylates CTD. The strength of the radioactive signals in the anti-FLAG antibody-immunoprecipitated fraction from *cdkc;2-2* was not affected by BML-259 treatment (**Fig. 4A**), but BML-259 inhibited phosphorylation of both GST-CTD and CDKC;2-FLAG in a dose-dependent manner (**Fig. 4A**). 10 μM BML-259 almost completely eliminated the phosphorylation signals of GST-CTD and CDKC;2-FLAG in the sample containing the immunocomplex. This concentration of BML-259 was lower than the effective concentration for period lengthening (**Fig. 1**), supporting the hypothesis that BML-259 lengthens circadian periods by inhibiting CDKC;2 kinase activity. The BML-259 analogs **1a, 1c, 1d, 1e** and **2** also inhibited kinase activity, whereas **1b** and **1f** did not (**Fig. 4B**). The structure–activity relationship for the kinase inhibitory activity in vitro is comparable to that for period lengthening in vivo (**Fig. 2**), which also supports the CDKC;2 kinase activity inhibition hypothesis.

To further understand the presumptive inhibitory mechanism(s) of BML-259 against CDKC;2, we performed molecular docking and molecular dynamics (MD) simulations (**Fig. 3C**) (Uehara et al. 2015). Because the crystal structures of Arabidopsis CDKC;2 and its partner cyclin CYCT have not yet been reported, the crystal structure (PDB ID: 3BLR; Baumli et al. 2008) of the human CDK9/cyclin T1 complex was used as the target protein in silico. Human CDK9 and cyclin T1 have similar sequences and functions to Arabidopsis CDKC;2 and its cyclin protein (Wang et al. 2014). The computational simulations predicted that the binding conformation of BML-259 would be in the ATP-binding pocket of CDK9 (**Fig. 4C**). The binding energy between CDK9 and BML-259 was calculated to be −7.84 kcal mol^{-1} (**Fig. 4C**). The binding energies for three of the BML-259 analogs with CDK9 were predicted to be −8.08, −5.56 and −5.98 kcal mol^{-1} for analogs **1a, 1b** and **1f**, respectively. These results suggested that BML-259 and analog **1a** should bind well to CDK9, compared to non-active analogs **1b** and **1f**.

The in silico model predicts that BML-259 binds to CDK9 through two hydrogen bonds to the main chain of Cys106, which is the hinge region in the ATP-binding pocket (**Fig. 4C**). Although Cys106 in human CDK9 corresponds to Met121 in CDKC;2, hydrogen bonding with BML-259 is likely between the main chain of Met121 and BML-259 in CDKC;2 (highlighted in **Supplementary Fig. S12**). One of the hydrogen bonds cannot be formed between **1f** and CDK9, due to N-methylation at the amide N-H bond of **1f**, which is compatible to weak

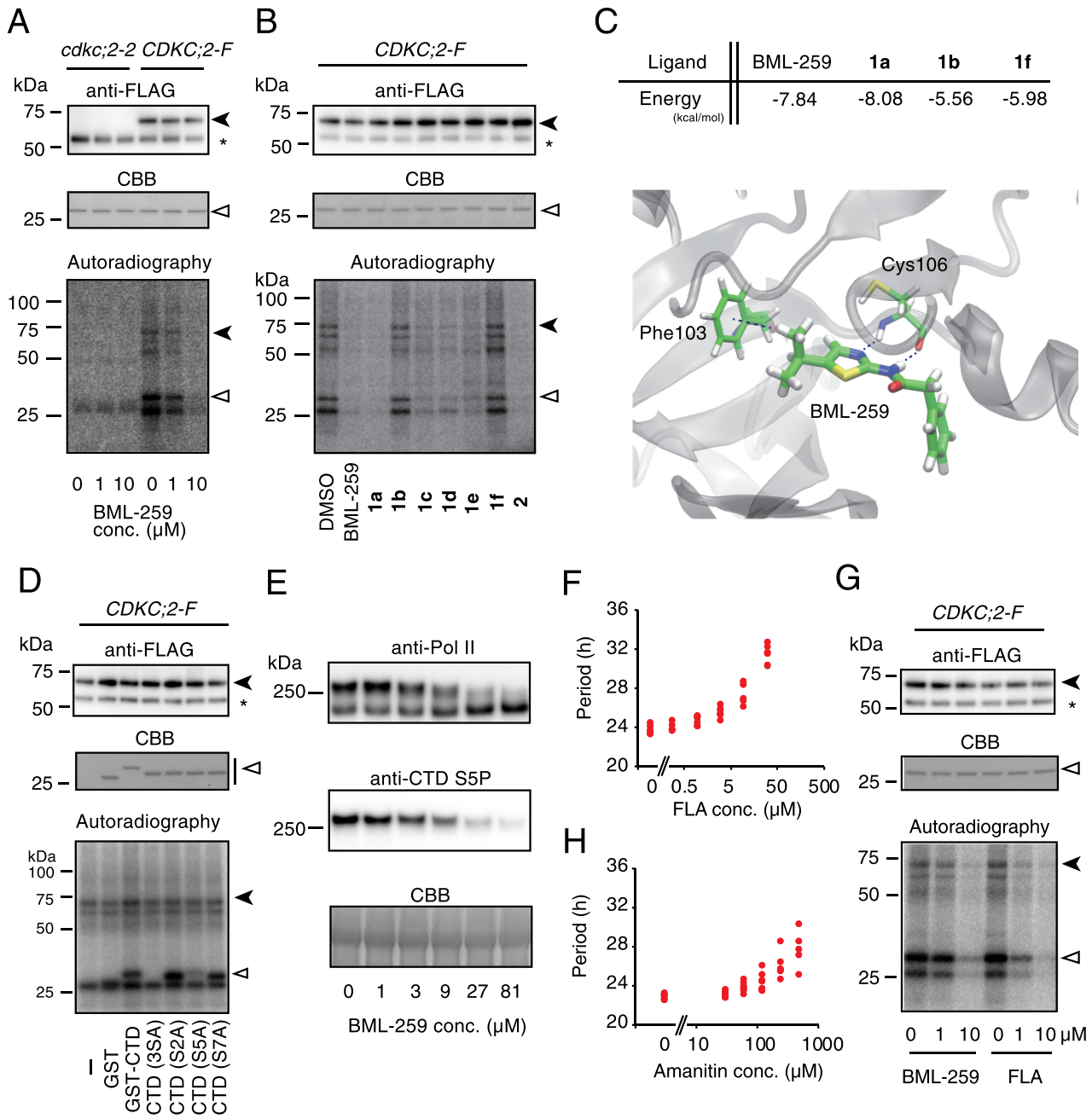

Fig. 4 Inhibition of Pol II phosphorylation lengthens the circadian period. (A) Phosphorylation of GST-CTD (white triangle) by the CDKC;2-FLAG immunocomplex (black arrowhead) (bottom panel). Top and middle panels are western blots with anti-FLAG antibody for CDKC;2-FLAG and Coomassie Brilliant Blue (CBB) staining for GST-CTD. The asterisk indicates anti-FLAG Antibody. (B) Structure–activity relationship of BML-259 and structural analogs with kinase inhibitory activity of CDKC;2 immunocomplex. Active inhibitors decrease kinase activity of the CDKC;2 immunocomplex. (C) In silico-predicted CDK9-ligand binding energies (kcal/mol). Larger negative value of binding energy is regarded as stronger binding affinity to CDK9 (upper). In silico-predicted binding structure of BML-259 in the human CDK9 ATP-binding pocket (lower). The positions of Phe103 and Cys106 of CDK9 are shown relative to BML-259. Blue, red and yellow represent nitrogen, oxygen and sulfur atoms, respectively. The dashed line between CDK9 Phe103 and BML-259 indicates a CH/π bond. Dashed lines between Cys106 and BML-259 represent hydrogen bonds. (D) Determination of phosphorylated CTD amino acid residues by CDKC;2. Mutated Ser5 was less phosphorylated by CDKC;2 immunocomplex. (E) RNA Pol II phosphorylation in plants treated with BML-259. Top panel: anti-Pol II antibody binds to hyper-phosphorylated (upper) and hypo-phosphorylated (lower) bands. Middle panel: Western blotting with anti-CTD S5P antibody. Bottom panel: CBB staining. (F) Dose-dependent period lengthening of *CCA1:LUC* treated with flavopiridol (FLA) ($n = 5$–8). (G) The CDKC;2 immunocomplex kinase activity with FLA in vitro. The black arrowhead and white triangle indicate the corresponding sizes of CDKC;2-FLAG and GST-CTD. (H) Period length of *CCA1:LUC* treated with amanitin ($n = 5$–8).

CDKC;2 inhibitory activity of **1f** (**Fig. 4B, C**). The isopropyl group at the thiazole C5 position of BML-259 forms a CH/π bond to CDK9 Phe103, which is also conserved as Phe118 in CDKC;2 (**Supplementary Fig. S12**). This bond is also found between **1a** and CDK9, but not between **1b** and CDK9, which may explain the weak CDKC;2 inhibitory activity of **1b** (**Fig. 4B, C**).

BML-259 attenuates Pol II Ser5 phosphorylation in vivo

The site-specific phosphorylation of CTD is correlated with Pol II activities (Zhu et al. 2018). For instance, an unphosphorylated form of Pol II accumulates downstream of the transcription start site, the Ser5 phosphorylated form associates with spliceosomes and the Ser2 phosphorylated form is enriched downstream of polyadenylation sites (Zhu et al. 2018).

To examine which amino acid residue(s) of CTD can be phosphorylated by CDKC;2, a phosphorylation assay using CDKC;2-FLAG immunocomplex was performed using recombinant GST-CTD substituted with Ara at Ser2, Ser5 and Ser7 [CTD (3SA)]. GST-CTD, but not CTD (3SA), was phosphorylated by the immunocomplex (**Fig. 4D**). Mutated CTD at Ser2 and Ser7 (CTD (S2A) and CTD (S7A), respectively) were phosphorylated, whereas the phosphorylation signal corresponding to CTD (S5A) was faint, suggesting that CDKC;2-FLAG immunocomplex phosphorylates CTD at Ser5 (**Fig. 4D**).

The phosphorylation state of Pol II CTD during the day–night cycle was assayed in vivo as a preliminary step in understanding how the clock and CTD phosphorylation relate. Total protein was extracted from wild-type seedlings grown under 12-h light/12-h dark conditions. There were no diurnal changes in bands detected by anti-Pol II or anti-CTD S5P antibodies (**Supplementary Fig. S13**), suggesting that CTD Ser5 phosphorylation is not strongly regulated during the diurnal cycle. We next examined whether BML-259 treatment for 1 h affect Pol II phosphorylation (**Fig. 4E**). Western blotting with anti-Pol II antibody revealed that treatment with BML-259 resulted in a decrease in intensity of the upper band of Pol II and increased lower band intensity, corresponding to hyper-phosphorylated and hypo-phosphorylated Pol II, respectively (**Fig. 4E**). Western blotting using anti-CTD S5P antibody confirmed that there was a decrease in CTD Ser5 phosphorylation with BML-259 treatment (**Fig. 4E**). Effective BML-259 dephosphorylation concentrations were similar to effective period lengthening concentrations.

Pharmacological inhibition of RNA polymerase II results in period lengthening

The pan-CDK inhibitor flavopiridol (FLA) is an inhibitor of Pol II phosphorylation. Its effects on circadian period were analyzed to confirm that phosphorylation of Pol II by CDKC;2 is involved in determining circadian period length. *CCA1:LUC* seedlings treated with FLA, which inhibits phosphorylation of Pol II Ser2 and Ser5 in vivo (Zhu et al. 2018), had significantly longer periods than untreated controls (**Fig. 4F**) (Ma et al. 2018). FLA also decreased the phosphorylation signals of Pol II, as had been demonstrated previously (**Supplementary Fig. S14**) (Zhu et al. 2018). Although FLA decreases phosphorylation of CTD (Zhu et al. 2018), it was unclear whether FLA would directly inhibit Arabidopsis CDKC;2 activity. We found that FLA inhibits kinase activity in the CDKC;2 immunocomplex in vitro (**Fig. 4G**), indicating that FLA decreases Pol II phosphorylation through inhibition of CDKC;2, and that Pol II phosphorylation is required for maintaining period length.

An inhibitor of transcription, amanitin, lengthened circadian period in a dose-dependent manner (**Fig. 4H**), suggesting that inhibition of the Pol II elongation step results in period lengthening. The period lengthening effects of FLA and amanitin were less than that of BML-259, suggesting that BML-259 lengthens periodicity through some mode of action in addition to phosphorylation of Pol II. It is also possible that other factors such as bioavailability and metabolic turnover of FLA and amanitin result in lower activities than with BML-259 treatment.

Conclusion

We used a chemical screening approach and found a period lengthening molecule, BML-259. Further experiments demonstrated that Arabidopsis *CDKC* is required for maintaining period length, an indispensable feature of the clock. The period lengthening effects of single *CDKC;2* mutations were less apparent than in clock gene mutants identified by genetic screening (Somers et al. 2000, Strayer et al. 2000, Martin-Tryon and Harmer 2008, Hong et al. 2010, Sanchez et al. 2010), and *CDKC;1* and *CDKC;2* are essential for growth (**Supplementary Fig. S8**) (Cui et al. 2007), highlighting the difficulties of using an exclusively forward genetic approach for finding and dissecting out involvement of *CDKC* genes in period maintenance.

Mode of actions of bioactive molecules in plants were mainly revealed by a candidate approach or screening for molecule-resistant mutants (De Rybel et al. 2009, Park et al. 2009, Noutoshi et al. 2012, Nakano et al. 2018), likely due to lack of implementation of technologies that had been taken in drug discovery field (Dejonghe and Russinova 2017). In this study, we employed the affinity-proteomic approach using the molecular probe and found that BML-259 preferentially binds to CDKC than other kinases in Arabidopsis. Furthermore, in silico simulations suggested that BML-259 acts as an ATP competitor for CDKC activity.

Materials and Methods

Screening for small molecules that alter the circadian period

Arabidopsis thaliana accession Col-0 was used as the wild-type. *CCA1:LUC* (Col-0) (Nakamichi et al. 2005) seeds were surface sterilized with 2.5% hypochlorous acid and plated on half-strength Murashige Skoog (MS) media. Seeds were kept at 4°C in the dark for 2 d, then transferred to constant 22°C and 12-h light/12-h dark conditions (LD). Four days after incubation, young

seedlings were transferred to 96-well plates with a dropper. Seedlings were treated with 50 μM of small molecules from the SCREEN-WELL® Kinase Inhibitor Library (BML-2832-0500, Enzo Life Sciences), which contain 80 known mammal kinase inhibitors, and 500 μM luciferin (120-05114, Wako) and incubated under LD conditions for 1 d before determining luminescence in real time (CL96, Churitsu, Toyoake, Japan). Light intensity during luminescence monitoring was 13–16 μmol m^{-2} s^{-1}. Wavelength of the light during luminescence monitoring is shown in **Supplementary Fig. S16**. Circadian rhythms based on expression of the luminescence reporter were calculated as previously reported (Kamioka et al. 2016). One molecule, BML-259, that significantly changed the circadian period was further investigated by dose–response experiments. *TOC1:LUC* (Col-0) (Uehara et al. 2019) was used to confirm the effect of BML-259 on the clock.

RNAseq analysis of Arabidopsis treated with BML-259

Sixteen 5-day-old Arabidopsis Col-0 seedlings grown on half-strength MS containing 2% sucrose under constant light conditions at 22°C were transferred into half-strength MS liquid with 2% sucrose containing BML-259 or DMSO as a sham control in a 35-mm-diameter dish. After 3-h incubation under white light at 22°C, seedlings were frozen in liquid nitrogen. We used three biological replicates for each experiment. RNA isolation and generation of RNAseq libraries were performed as reported previously (Kamioka et al. 2016). Deep sequencing was performed with Illumina NextSeq 500 according to the supplier's protocol (Illumina). Only sequence reads exceeding 50 continuous nucleotides with quality values >25 were used, and further procedures, such as mapping to TAIR10 transcripts and read counts normalization to counts per million (CPM) (Dataset S1-A), were performed as previously reported (Kamioka et al. 2016). The significance of expression changes between DMSO- and 27 μM BML-259-treated samples was determined by calculation of FDR using Edge-R (Robinson et al. 2010). Genes whose expression in plants treated with 27 μM BML-259 were different from those in plants treated with DMSO (FDR $q < 10^{-10}$ and > 10-fold change) were annotated as 'up-regulated genes (Dataset S1-B)' or 'down-regulated genes (Dataset S1-C)' by Edge-R (Robinson et al. 2010). Unchanged genes between 27 μM BML-259 and DMSO treatments were also determined (FDR $q > 0.5$) (Dataset S1-D). Volcano plot was generated by R (**Fig. 1F**). Mean CPM of three biological replicates was used, and the maximal CPM of each gene was set to the relative value of '1' to make up the heat map (**Fig. 1G**). Peak time of gene expression for **Fig. 1G** was calculated using the Phaser tool with the condition = LL12_LDHH and the correction cutoff value = 0.8 (http://www.mocklerlab.org/tools) (Mockler et al. 2007). Rhythmic genes and non-rhythmic genes in **Fig. 1H** and **I** were obtained from the Phaser tool with the condition = LL12_LDHH and the correction cutoff value = 0.8. Circadian phases of 4,554 down-regulated genes by BML-259 were examined by the Phaser tool with the condition = LL12_LDHH and the correction cutoff value = 0.8. eGO analyses for genes up- or down-regulated by treatment with 27 μM BML-259 compared to a DMSO control (Dataset S1) were performed in the Arabidopsis Information Resource (TAIR) (https://www.arabidopsis.org/tools/go_term_enrichment.jsp), using default settings. RNAseq data from BML-259-treated Arabidopsis have been deposited in the DDBJ Sequence Read Archive (http://trace.ddbj.nig.ac.jp/dra/index_e.html) with accession number DRA009508.

Synthesis of BML-259 analogs

Synthesis strategy and structure validation of BML-259 analogs are described in **Supplementary note 1.**

Target identification

Two-week-old seedlings to be used for pull-down assays (~1 g) were grown under LD conditions until harvest at ZT0, 6, 12 and 18 and stored at −80°C until use. Seedlings from each of the separate time points were mixed and ground to powder in liquid nitrogen. About 1 g of the powdered tissue was transferred to a 15-ml tube, lysed in 10 ml lysis buffer A [150 mM Tris-HCl pH 7.5, 15 mM $MgCl_2$, 15 mM ethylene glycol tetraacetic acid (EGTA), 1 mM dithiothreitol (DTT), protease inhibitor mixture (P9599; Sigma-Aldrich) and 50 μM 26S protease inhibitor MG132 (C2211; Sigma-Aldrich)] and then sonicated (VCX-130PB, Sonics and Materials) five times at 50–70% output for 10 sec. After sonication, 60 μl of 10% (v/v) NP40 was added to each tube (0.1%, final concentration). Samples were incubated on ice for 5 min and centrifuged at 13,000 g at 4°C for 10 min. Protein samples (3 mg) were incubated with or without 50 μM BML-259 (0.5% DMSO, final concentration) at 4°C for 30 min with rotary mixing. A 250 μl aliquot of BML-beads suspended in PBS was washed 3× with beads buffer [100 mM Tris-HCl pH 7.5, 250 mM NaCl, 5 mM ethylenediaminetetraacetic acid, 5 mM EGTA, 0.1% (v/v) NP40, protease inhibitor mixture and 50 μM 26S protease inhibitor MG132] and re-suspended in 250 μl of beads buffer. BML-beads were equally divided into two tubes and added to cell lysates that had been incubated with or without BML-259. Samples were gently rotated at 4°C for 1 h. BML-beads resins were washed with beads buffer six times and suspended in sodium dodecyl sulfate (SDS) sample buffer and then boiled at 95°C for 8 min. Supernatants were collected for proteomic analysis.

SDS-PAGE and in-gel digestion of protein samples

After boiling protein-bound BML-beads in SDS sample buffer, released proteins were partially separated (~2 cm) using a Laemmli SDS-PAGE slab gel. Each lane was divided into six pieces, with about 0.2 cm^3 of each piece. In-gel digestion was performed according to the method described by Rosenfeld et al. (1992).

Mass spectroscopy, chromatographic methods, instrumentation and analysis

Samples were analyzed by nano-flow reverse-phase liquid chromatography followed by tandem MS, using a Q Exactive Hybrid Quadrupole-Orbitrap Mass Spectrometer (ThermoFisher Scientific). The capillary reverse-phase high performance liquid chromatography-mass spectrometry (MS)/MS system was composed of a Dionex U3000 gradient pump equipped with a VICI CHEMINERT valve and a Q Exactive equipped with a Dream Spray nano-electrospray ionization (NSI) source (AMR, Tokyo, Japan). Samples were automatically injected using a PAL System autosampler (CTC Analytics, Zwingen, Switzerland) and a peptide L-trap column (Trap and Elute mode, Chemical Evaluation Research Institute, Tokyo) attached to an injector valve for desalinating and concentrating peptides. After washing the trap with MS-grade water containing 0.1% (v/v) trifluoroacetic acid and 2% (v/v) acetonitrile (solvent C), the peptides were loaded onto a separation capillary C18 reverse-phase column (NTCC-360/100-3-125, 125 × 0.1 mm, Nikkyo Technos, Tokyo). The mobile phases were as follows: A, 100% water containing 0.5% (v/v) acetic acid, and B, 80% (v/v) acetonitrile containing 0.5% (v/v) acetic acid. The column was developed at a flow rate of 0.5 μL min^{-1} with an acetonitrile concentration gradient of 5% B to 35% B for 20 min, then 35% B to 95% B for 1 min, 95% B for 3 min, 95% B to 5% B for 1 min, and finally re-equilibrating with 5% B for 10 min. Xcalibur 3.0.63 (ThermoFisher Scientific) was used to record peptide spectra over a mass range of m/z 350–1,500. MS spectra were recorded followed by 20 data-dependent high-energy collisional dissociation (HCD) MS/MS spectra generated from the 20 highest intensity precursor ions. Multiply-charged peptides were chosen for MS/MS experiments due to their good fragmentation characteristics. MS/MS spectra were interpreted, and peak lists were generated using Proteome Discoverer 2.0.0.802 (ThermoFisher Scientific). Proteomic searches were performed using SEQUEST (ThermoFisher Scientific) against the *Arabidopsis thaliana* (TAIR TaxID = 3702) peptide sequence database. Search parameters were set as follows: enzyme selected with two maximum missing cleavage sites, a mass tolerance of 10 ppm for peptide tolerance, 0.02 Da for MS/MS tolerance, fixed modification of carbamidomethyl (C) and variable modification of oxidation (M). Peptide identifications were based on significant Xcorr

values (high confidence filter). Peptide identification and modification information returned from SEQUEST were manually inspected and filtered to obtain confirmed peptide identification and modification lists of HCD MS/MS. We performed target ID using different biological samples (Experiment 2) to validate the initial screening. Only reproducibly BML-259-beads-binding proteins (at least three unique peptides without competitor sample in both experiment, and enrichment of unique peptide were more than 10 times higher in without competitor sample compared to competitor sample) are shown in **Fig. 2C**.

Phylogenic analysis

Amino acid sequences of Arabidopsis CDK were obtained from TAIR (http://www.arabidopsis.org/) or UniPort (https://www.uniprot.org/uniprot/). Human sequences were from UniProt or NCBI (https://www.ncbi.nlm.nih.gov) with the following IDs: CDK1 (P06493), CDK2 (P24941), CDK3 (Q00526), CDK4 (P11802), CDK5 (CAG33322.1), CDK6 (NP_001250.1) CDK7 (AIC62961.1), CDK8 (CAA59754.1), CDK9 (AAF72183.1), CDK10a (Q15131), CDK11a (Q9UQ88), CDK12 (Q9NYV4), CDK13 (Q14004), CDK14 (O94921), CDK15 (Q96Q40), CDK16 (Q00536), CDK17 (Q00537), CDK18 (Q07002), CDK19 (Q9BWU1), CDK20 (Q8IZL9), CDKA;1 (P24100), CDKB;1 (P25859), CDKC;1 (AT5G10270), CDKC;2 (AT5G64960), CDKD;1 (Q9C9U2), CDKE;1 (Q84TI6), CDKF;1 (O80345) and CDKG;1 (Q9FGW5).

Evolutionary analyses were conducted in MEGA7 (7) (**Supplementary Fig. S6**). An evolutionary history was inferred using the Neighbor-Joining method (Saitou and Nei 1987). The optimal tree with the sum of branch length = 6.21746923 is shown. The percentage of replicate trees in which the associated taxa clustered together in the bootstrap test with 500 replicates is shown next to the nodes (Felsenstein 1985). The tree is drawn to scale, with branch lengths in the same units as those of the evolutionary distances used to infer the phylogenetic tree. Evolutionary distances were computed using the Poisson correction method (Zuckerkandl and Pauling 1965) and are expressed as the number of amino acid substitutions per site. The analysis involved 28 amino acid sequences. All positions containing gaps and missing data were eliminated (complete deletion). There were a total of 190 positions in the final dataset (Kumar et al. 2016). ClustalW2.1 was used to generate the alignment of CDK9, CDKC;1 and CDKC;2 (http://clustalw.ddbj.nig.ac.jp/index.php?lang=en) (**Supplementary Fig. S12**).

Generation of mutant and transgenic plants

The *cdkc;2-2* line (SALK_029546.51.85.x) was obtained from the Arabidopsis Biological Resource Center. No full-length *CDKC;2* mRNA was detected in the *cdkc;2-2* by RT-PCR, confirming that the allele is a null mutant as previously demonstrated (Wang et al. 2014). The *cdkc;2-2* mutant line was crossed with *CCA1:LUC* transgenic plants to generate *cdkc;2-2/CCA1:LUC*. CRISPR-Cas9-mediated genome editing (Tsutsui and Higashiyama 2017) was used to make *cdkc;2-cr1* and *cdkc;2-cr2* mutants. The DNA oligonucleotides targeting *CDKC;2* were treated with T4 polynucleotide kinase (2021S, Takara, Kyoto) and annealed with each other. Annealed DNA was diluted with H_2O to 1/250 and ligated to AarI-treated (ER1581, Thermo Fisher Scientific) pKIR1.1 (Tsutsui and Higashiyama 2017) with Instant Sticky-end Ligase Master Mix (M0370S, New England BioLabs) to generate pKIR1.1*CDKC;2*. These constructs were transformed into *CCA1:LUC* plants with an *Agrobacterium tumefaciens*-mediated method (Bechtold et al. 1993). T1 plants were screened by searching for red fluorescence in the seeds, since the pKIR1.1 vector harbors an OLE1-RFP marker (Tsutsui and Higashiyama 2017). T1 seeds were then sown in soil and T2 seeds were harvested. Seeds not harboring the Cas9 cassette were counter-selected by the absence of red fluorescence to avoid further off-target genome editing. DNA sequences around the CRISPR-*CDKC;2* target were confirmed by Sanger sequencing. Two different alleles of *cdkc;2* were named as *cdkc;2-cr1* and *cdkc;2-cr2* (**Fig. 3A**). To generate *CDKC;2pro:CDKC;2-FLAG/cdkc;2-2/CCA1:LUC*, a region containing the *CDKC;2* promoter and coding sequence was amplified with KOD-Plus-Neo DNA polymerase (KOD-401, Toyobo) from Col-0 genomic DNA. Resultant amplicon was cloned into pENTR/D-TOPO (K240020, ThermoFisher), to generate pENTR/D-*CDKC;2pro:CDKC;2*. The DNA sequence of pENTR/D-*CDKC;2pro:CDKC;2* was validated by Sanger sequencing. The pENTR/D-*CDKC;2pro:CDKC;2* plasmid was incubated with Gateway LR clonase II (11791-020, ThermoFisher) and modified pBA-PF5 binary vector (Kamioka et al. 2016), to generate a C-terminal 3xFLAG fusion construct (pBA-*CDKC;2pro:CDKC;2-FLAG*). The pBA-*CDKC;2pro:CDKC;2-FLAG* was transferred into the *cdkc;2-2/CCA1:LUC* line by *Agrobacterium* as previously described (Kamioka et al. 2016). Expression of CDKC;2-FLAG protein of an appropriate size was found in four independent T1 plants (#1–#4), by western blotting with anti-FLAG antibody as described previously (Kamioka et al. 2016). The T3 generation of transformants #1 and #2 was used in this study.

Two different alleles of *cdkc;1* (*cdkc;1-cr1* and *cdkc;1-cr2*) were obtained with the CRISPR Cas9 vector pKIR1.1-*CDKC;1* using *CCA1:LUC* as a parental plant (**Fig. 3E**). Two guide RNAs were cloned into pKIR1.1 using an endogenous tRNA-processing system method (Xie et al. 2015, Toda et al. 2019). The two *cdkc;1* alleles have premature termination codons in the kinase domain. *cdkc;1-cr1* was crossed with *cdkc;2-2*, to make the *cdkc;1 cdkc;2* double loss-of-function mutants, but double loss-of-function mutants were nonviable. A *cdkc;2-2* homozygous *cdkc;1-cr1* heterozygous plant grew abnormally, and its seed maturation rate of *cdkc;2-2* heterozygous *cdkc;1-cr1* homozygous was reduced to 60–80% of the *cdkc;1-cr1* or *cdkc;2-2* parental types (**Supplementary Fig. S8**), suggesting an essential role for *CDKC*.

To simultaneously knock down *CDKC;1* and *CDKC;2*, 400 bp of *CDKC;1* (from 529 to 928 bp in the *CDKC;1* coding sequence) was cloned in pENTR/D-TOPO, generating pENTR/D-CDKC-RNAi-1 (**Supplementary Fig. S9**). pENTR/D-CDKC-RNAi-1 was treated with LR clonase and pFAST-03R (VIB-UGENT Center for Plant Systems Biology) (Shimada et al. 2010), to generate pFAST-03R-CDKC-RNAi-1. The vector was transformed into *CCA1:LUC* plants by an *Agrobacterium*-mediated method. The *CCA1:LUC* luminescence of T1 seeds harboring the RFP marker was measured (**Supplementary Fig. S9**). After the luminescence assay, representative seedlings were grown, and expression of *CDKC;1* and *CDKC;2* was determined. Expression of *IPP2* was tested as a non-target gene of CDKC-RNAi-1. RFP-positive T2 seeds of two knockdown lines (B07 and C08) were selected to examine *CCA1:LUC* luminescence (**Fig. 3H**). CDKC-RNAi-2 harboring 1–400 bp of *CDKC;1* was tested as another construct for knockdown of *CDKC;1* and *CDKC;2* (**Supplementary Fig. S9**). The *CCA1:LUC* circadian rhythm period and *CDKC;1* and *CDKC;2* expression of T1 plants harboring pFAST-03R-CDKC-RNAi-2 were examined with control T1 plants transformed with pFAST-03R empty vector (**Supplementary Fig. S9**).

Circadian rhythm assays with mutants and small molecules

The circadian rhythms of *cdkc;2-2/CCA1:LUC*, *cdkc;2-cr1/CCA1:LUC*, *cdkc;2-cr2/CCA1:LUC*, *CDKC;2pro:CDKC;2-FLAG/cdkc;2-2/CCA1:LUC*, *cdkc;1-cr1/CCA1:LUC*, *cdkc;1-cr2/CCA1:LUC* and *CDKC RNAi-1/ CCA1:LUC* (lines B07 and C08) plants were analyzed with Col-0 *CCA1:LUC* as control, as previously described (Kamioka et al. 2016). Circadian rhythm assays for plants treated with pan-CDK (FLA, [CS-0018, Chemscence]) or the Pol II inhibitor (alpha-Amanitin [010-22961, Wako]) used 4-day-old *CCA1:LUC* seedlings grown under LD conditions. 20 µl MS liquid medium containing 2% sucrose, 500 µM D-Luciferin potassium salt (120-05114, Wako) and small molecules at different concentrations was added to each well. Circadian periods of the *CCA1:LUC* reporter were measured and recorded as above.

Kinase activity of CDKC;2 purified from Arabidopsis

To make recombinant GST-CTD, the DNA sequence encoding a tandem repeat of Pol II CTD was generated by amplification of annealed oligo DNA (Dataset S2) with KOD-Plus-Neo (TOYOBO). Amplicons were cloned into pGEX-2T-

between the *Bam*HI and *Eco*RI sites, generating pGEX-CTD. The pGEX-CTD construct was validated by Sanger sequencing and transformed into *E. coli* BL21. The GST-CTD fusion protein was purified from BL21/pGEX-CTD, according to the supplier's protocol (GE Healthcare). GST-CTD (S2A), GST-CTD (S5A), GST-CTD (S7A) and GST-CTD (3SA) were purified by the same method. These GST-CTD proteins were used as substrates for CDKC;2. *CDKC;2pro:CDKC;2-FLAG/cdkc;2-2/CCA1:LUC* plants were grown under LD for 2 weeks, frozen at ZT2 and kept at −80°C until use. 2 g of frozen plant tissue was ground to powder in liquid nitrogen, and about 1 g of the powdered tissue was lysed in 5 ml of lysis buffer B [50 mM Tris-HCl, pH 7.5, 100 mM NaCl, 0.1% Trinton X-100, 50 μM MG132 (Sigma), protease inhibitor cocktail (Sigma)]. The sample was sonicated and kept on ice for 10 min, and the plant tissue was pelleted by centrifugation with 12,000 g for 10 min at 4°C. The supernatant was immunoprecipitated with anti-FLAG antibody (F3165, Sigma) Dynabeads Protein G (DB10003, Thermofisher), as described previously (Nakamichi et al. 2012). Immunoprecipitated CDKC;2-FLAG complex was then suspended in 500 μl of kinase reaction buffer [50 mM Tris-HCl pH 7.5, 10 mM $MgCl_2$, 0.5 mM DTT, 50 μM MG132, protease inhibitor cocktail] for western blotting, which confirmed immunoprecipitation of CDKC;2-FLAG. 23 μl of G-beads suspended in kinase reaction buffer was combined with 1 μl of recombinant GST-CTD and 1 μl of [γ-^{32}P] ATP (NNNEG502A, PerkinElmer) and kept at 37°C for 40 min, with mixing at 10-min intervals. The reaction was stopped by adding 10 μl of 3× SDS sample buffer and boiled for 5 min. Samples were resolved on Super Sep Ace 10–20% gradient gels (198-15041, Fujifilm-Wako). Dried gels were exposed on an imaging plate (BAS IP-MS 2040), and radioactive signals were detected with a Typhoon FLA 7000 Laser Scanner/Imager (GE Healthcare).

Pol II phosphorylation in vivo

To detect Pol II phosphorylation in Arabidopsis, 20 4-day-old Col-0 seedlings grown under 12h L/ 12h D conditions were harvested and frozen in liquid nitrogen at 2-h intervals. To detect Pol II phosphorylation in Arabidopsis seedlings treated with BML-259, 20 of 4-day old seedlings per treatment grown under constant light were soaked in different concentrations of inhibitor and vacuum infiltrated for 30 sec. Samples were kept under constant light for 1 h and flash-frozen with liquid nitrogen. Total proteins were extracted from seedlings as previously described (Mizoi et al. 2019). The protein samples were separated in a 6% acrylamide gel (195-15171, Fujifilm-Wako). Pol II was detected by anti-RNA Polymerase II antibody (MABI0601, Fujifilm-Wako). Phospho-S5 CTD was detected by anti-phospho RNA Polymerase II CTD (Ser5) (MABI0603, Fujifilm-Wako).

In silico analysis

Molecular docking simulations using the FlABCps method (Uehara et al. 2015) were applied to BML-259 and its analogs, where the crystal structure of human CDK9 and the cyclin T1 complex (PDB ID: 3BLR) (Baumli et al. 2008) were employed as target proteins. The energy score was evaluated with an AutoDock force field (Huey et al. 2007). We also performed 100 ns MD simulations of the ligand–protein complexes with a time step of 2 fs under NPT conditions at 300 K and 1 atm. A periodic boundary box (112 × 98 × 103 $Å^3$) for MD simulation was composed of human CDK9/cyclin T1, ligand (BML-259 or its analogs) and water molecules. The computational settings for molecular docking and MD simulations were the same as in a previous study (Fujimoto et al. 2018). All MD simulations were performed with the AMBER16 program software package (Case et al. 2016).

Supplementary Data

Supplementary data are available at *PCP* online.

Data Availability

The RNAseq data from BML-259-treated Arabidopsis reported in this article have been deposited in the DDBJ Sequence Read Archive (DRA, http://trace.ddbj.nig.ac.jp/dra/index_e.html) with accession number DRA009508.

Funding

Grant-in-Aid for Sci. Res. on Innovative Areas 18H04428 to J.Y., 20H05411 to N.N. and 15H05956 to T.K, K.K. and N.N.; Toyota Riken Scholar; NAGASE Science Technology Foundation; Takeda Science Foundation; Japan Society for the Promotion of Science KAKENHI grant (21H05656, 18H02136, 20K21272) to N.N; ITbM supported by the World Premier International Research Center (WPI) Initiative, Japan.

Acknowledgements

We thank S. Takao for part of chemical screening; Arabidopsis Biological Resource Center for *cdkc;2-2*, pKIR1.1 for T. Higashiyama; VIB-UGENT Center for Plant Systems Biology for pFAST-03R; and T. Kondo, K. Miwa, K. Terauchi, M. Nakajima, J. Tomita, T. Yamashino for helpful discussion.

Disclosures

The authors have no conflicts of interest to declare.

References

Baumli, S., Lolli, G., Lowe, E.D., Troiani, S., Rusconi, L., Bullock, A.N., et al. (2008) The structure of P-TEFb (CDK9/cyclin T1), its complex with flavopiridol and regulation by phosphorylation. *EMBO J.* 27: 1907–1918.

Bechtold, N., Ellis, J. and Pelletier, G. (1993) In planta Agrobacterium mediated gene transfer by infiltration of adult Arabidopsis thaliana plants. *C. R. Acad. Sci. Paris, Life Sci.* 316: 1194–1199.

Bosken, C.A., Farnung, L., Hintermair, C., Merzel Schachter, M., Vogel-Bachmayr, K., Blazek, D., et al. (2014) The structure and substrate specificity of human Cdk12/Cyclin K. *Nat. Commun.* 5: 3505.

Case, D., Betz, R., Cerutti, D.S., Darden, T., Duke, R., Giese, T.J., et al. (2016) Amber 16. University of California, San Francisco.

Chu, C., Geng, Y., Zhou, Y. and Sicinski, P. (2021) Cyclin E in normal physiology and disease states. *Trends Cell Biol.* 31: 732–746.

Cui, X., Fan, B., Scholz, J. and Chen, Z. (2007) Roles of Arabidopsis cyclin-dependent kinase C complexes in cauliflower mosaic virus infection, plant growth, and development. *Plant Cell* 19: 1388–1402.

De Rybel, B., Audenaert, D., Vert, G., Rozhon, W., Mayerhofer, J., Peelman, F., et al. (2009) Chemical inhibition of a subset of Arabidopsis thaliana GSK3-like kinases activates brassinosteroid signaling. *Chem. Biol.* 16: 594–604.

Dejonghe, W. and Russinova, E. (2017) Plant chemical genetics: from phenotype-based screens to synthetic biology. *Plant Physiol.* 174: 5–20.

Dibner, C., Sage, D., Unser, M., Bauer, C., d'Eysmond, T., Naef, F., et al. (2009) Circadian gene expression is resilient to large fluctuations in overall transcription rates. *EMBO J.* 28: 123–134.

Dodd, A.N., Salathia, N., Hall, A., Kevei, E., Toth, R., Nagy, F., et al. (2005) Plant circadian clocks increase photosynthesis, growth, survival, and competitive advantage. *Science* 309: 630–633.

Doherty, C.J. and Kay, S.A. (2010) Circadian control of global gene expression patterns. *Annu. Rev. Genet.* 44: 419–444.

Felsenstein, J. (1985) Confidence limits on phylogenies: an approach using the bootstrap. *Evolution* 39: 783–791.

Fujimoto, K.J., Nema, D., Ninomiya, M., Koketsu, M., Sadanari, H., Takemoto, M., et al. (2018) An in silico-designed flavone derivative, 6-fluoro-4-′-hydroxy-3 ′,5 ′-dimetoxyflavone, has a greater anti-human cytomegalovirus effect than ganciclovir in infected cells. *Antivir. Res.* 154: 10–16.

Helal, C.J., Sanner, M.A., Cooper, C.B., Gant, T., Adam, M., Lucas, J.C., et al. (2004) Discovery and SAR of 2-aminothiazole inhibitors of cyclin-dependent kinase 5/p25 as a potential treatment for Alzheimer's disease. *Bioorg. Med. Chem. Lett.* 14: 5521–5525.

Hong, S., Song, H.R., Lutz, K., Kerstetter, R.A., Michael, T.P. and McClung, C.R. (2010) Type II protein arginine methyltransferase 5 (PRMT5) is required for circadian period determination in Arabidopsis thaliana. *Proc. Natl. Acad. Sci. U.S.A.* 107: 21211–21216.

Huey, R., Morris, G.M., Olson, A.J. and Goodsell, D.S. (2007) A semiempirical free energy force field with charge-based desolvation. *J. Comput. Chem.* 28: 1145–1152.

Hung, F.Y., Chen, F.F., Li, C.L., Chen, C., Lai, Y.C., Chen, J.H., et al. (2018) The Arabidopsis LDL1/2-HDA6 histone modification complex is functionally associated with CCA1/LHY in regulation of circadian clock genes. *Nucleic Acids Res.* 46: 10669–10681.

Jones, M.A., Williams, B.A., McNicol, J., Simpson, C.G., Brown, J.W. and Harmer, S.L. (2012) Mutation of Arabidopsis spliceosomal timekeeper locus1 causes circadian clock defects. *Plant Cell* 24: 4066–4082.

Kamioka, M., Takao, S., Suzuki, T., Taki, K., Higashiyama, T., Kinoshita, T., et al. (2016) Direct repression of evening genes by CIRCADIAN CLOCK-ASSOCIATED1 in the Arabidopsis circadian clock. *Plant Cell* 28: 696–711.

Karakashian, M.W. and Hastings, J.W. (1962) The inhibition of a biological clock by actinomycin D. *Proc. Natl. Acad. Sci. U.S.A.* 48: 2130–2137.

Kumar, S., Stecher, G. and Tamura, K. (2016) MEGA7: molecular evolutionary genetics analysis version 7.0 for bigger datasets. *Mol. Biol. Evol.* 33: 1870–1874.

Lin, C. (2002) Blue light receptors and signal transduction. *Plant Cell* 14 Suppl: S207–S225.

Ma, Y., Gil, S., Grasser, K.D. and Mas, P. (2018) Targeted recruitment of the basal transcriptional machinery by LNK clock components controls the circadian rhythms of nascent RNAs in Arabidopsis. *Plant Cell* 30: 907–924.

Martin-Tryon, E.L. and Harmer, S.L. (2008) XAP5 CIRCADIAN TIMEKEEPER coordinates light signals for proper timing of photomorphogenesis and the circadian clock in Arabidopsis. *Plant Cell* 20: 1244–1259.

Mizoi, J., Kanazawa, N., Kidokoro, S., Takahashi, F., Qin, F., Morimoto, K., et al. (2019) Heat-induced inhibition of phosphorylation of the stress-protective transcription factor DREB2A promotes thermotolerance of Arabidopsis thaliana. *J. Biol. Chem.* 294: 902–917.

Mockler, T.C., Michael, T.P., Priest, H.D., Shen, R., Sullivan, C.M., Givan, S.A., et al. (2007) The DIURNAL project: DIURNAL and circadian expression profiling, model-based pattern matching, and promoter analysis. *Cold Spring Harb. Symp. Quant. Biol.* 72: 353–363.

Nakajima, M., Imai, K., Ito, H., Nishiwaki, T., Murayama, Y., Iwasaki, H., et al. (2005) Reconstitution of circadian oscillation of cyanobacterial KaiC phosphorylation in vitro. *Science* 308: 414–415.

Nakajima, M., Koinuma, S. and Shigeyoshi, Y. (2015) Reduction of translation rate stabilizes circadian rhythm and reduces the magnitude of phase shift. *Biochem. Biophys. Res. Commun.* 464: 354–359.

Nakamichi, N., Kiba, T., Kamioka, M., Suzuki, T., Yamashino, T., Higashiyama, T., et al. (2012) Transcriptional repressor PRR5 directly regulates clock-output pathways. *Proc. Natl. Acad. Sci. U.S.A.* 109: 17123–17128.

Nakamichi, N., Kita, M., Ito, S., Yamashino, T. and Mizuno, T. (2005) PSEUDO-RESPONSE REGULATORS, PRR9, PRR7 and PRR5, together play essential roles close to the circadian clock of Arabidopsis thaliana. *Plant Cell Physiol.* 46: 686–698.

Nakano, T., Tanaka, S., Ohtani, M., Yamagami, A., Takeno, S., Hara, N., et al. (2018) FPX is a novel chemical inducer that promotes callus formation and shoot regeneration in plants. *Plant Cell Physiol.* 59: 1555–1567.

Nohales, M.A. and Kay, S.A. (2016) Molecular mechanisms at the core of the plant circadian oscillator. *Nat. Struct. Mol. Biol.* 23: 1061–1069.

Noutoshi, Y., Okazaki, M., Kida, T., Nishina, Y., Morishita, Y., Ogawa, T., et al. (2012) Novel plant immune-priming compounds identified via high-throughput chemical screening target salicylic acid glucosyltransferases in arabidopsis. *Plant Cell* 24: 3795–3804.

Ong, W.D., Okubo-Kurihara, E., Kurihara, Y., Shimada, S., Makita, Y., Kawashima, M., et al. (2017) Chemical-induced inhibition of blue light-mediated seedling development caused by disruption of upstream signal transduction involving cryptochromes in Arabidopsis thaliana. *Plant Cell Physiol.* 58: 95–105.

Ono, A., Sato, A., Fujimoto, K.J., Matsuo, H., Yanai, T., Kinoshita, T., et al. (2019) 3,4-dibromo-7-azaindole modulates Arabidopsis circadian clock by inhibiting casein kinase 1 activity. *Plant Cell Physiol.* 60: 2360–2368.

Park, S.Y., Fung, P., Nishimura, N., Jensen, D.R., Fujii, H., Zhao, Y., et al. (2009) Abscisic acid inhibits type 2C protein phosphatases via the PYR/PYL family of START proteins. *Science* 324: 1068–1071.

Robinson, M.D., McCarthy, D.J. and Smyth, G.K. (2010) edgeR: a Bioconductor package for differential expression analysis of digital gene expression data. *Bioinformatics* 26: 139–140.

Rosenfeld, J., Capdevielle, J., Guillemot, J.C. and Ferrara, P. (1992) In-gel digestion of proteins for internal sequence analysis after one- or two-dimensional gel electrophoresis. *Anal. Biochem.* 203: 173–179.

Saito, A.N., Matsuo, H., Kuwata, K., Ono, A., Kinoshita, T., Yamaguchi, J., et al. (2019) Structure-function study of a novel inhibitor of the casein kinase 1 family in Arabidopsis thaliana. *Plant Direct* 3: e00172.

Saitou, N. and Nei, M. (1987) The neighbor-joining method: a new method for reconstructing phylogenetic trees. *Mol. Biol. Evol.* 4: 406–425.

Sanchez, S.E., Petrillo, E., Beckwith, E.J., Zhang, X., Rugnone, M.L., Hernando, C.E., et al. (2010) A methyl transferase links the circadian clock to the regulation of alternative splicing. *Nature* 468: 112–116.

Shalit-Kaneh, A., Kumimoto, R.W., Filkov, V. and Harmer, S.L. (2018) Multiple feedback loops of the Arabidopsis circadian clock provide rhythmic robustness across environmental conditions. *Proc. Natl. Acad. Sci. U.S.A.* 115: 7147–7152.

Shimada, T.L., Shimada, T. and Hara-Nishimura, I. (2010) A rapid and non-destructive screenable marker, FAST, for identifying transformed seeds of Arabidopsis thaliana. *Plant J.* 61: 519–528.

Somers, D.E., Devlin, P.F. and Kay, S.A. (1998) Phytochromes and cryptochromes in the entrainment of the Arabidopsis circadian clock. *Science* 282: 1488–1490.

Somers, D.E., Schultz, T.F., Milnamow, M. and Kay, S.A. (2000) ZEITLUPE encodes a novel clock-associated PAS protein from Arabidopsis. *Cell* 101: 319–329.

Strayer, C., Oyama, T., Schultz, T.F., Raman, R., Somers, D.E., Mas, P., et al. (2000) Cloning of the Arabidopsis clock gene TOC1, an autoregulatory response regulator homolog. *Science* 289: 768–771.

Toda, E., Koiso, N., Takebayashi, A., Ichikawa, M., Kiba, T., Osakabe, K., et al. (2019) An efficient DNA- and selectable-marker-free genome-editing system using zygotes in rice. *Nat. Plants* 5: 363–368.

Tong, M., Lee, K., Ezer, D., Cortijo, S., Jung, J., Charoensawan, V., et al. (2020) The Evening Complex establishes repressive chromatin domains via H2A.Z deposition. *Plant Physiol.* 182: 612–625.

Tsutsui, H. and Higashiyama, T. (2017) pKAMA-ITACHI vectors for highly efficient CRISPR/Cas9-mediated gene knockout in Arabidopsis thaliana. *Plant Cell Physiol.* 58: 46–56.

Uehara, S., Fujimoto, K.J. and Tanaka, S. (2015) Protein-ligand docking using fitness learning-based artificial bee colony with proximity stimuli. *Phys. Chem. Chem. Phys.* 17: 16412–16417.

Uehara, T.N., Mizutani, Y., Kuwata, K., Hirota, T., Sato, A., Mizoi, J., et al. (2019) Casein kinase 1 family regulates PRR5 and TOC1 in the Arabidopsis circadian clock. *Proc. Natl. Acad. Sci. U.S.A.* 116: 11528–11536.

Wang, L., Kim, J. and Somers, D.E. (2013) Transcriptional corepressor TOPLESS complexes with pseudoresponse regulator proteins and histone deacetylases to regulate circadian transcription. *Proc. Natl. Acad. Sci. U.S.A.* 110: 761–766.

Wang, Z.W., Wu, Z., Raitskin, O., Sun, Q. and Dean, C. (2014) Antisense-mediated FLC transcriptional repression requires the P-TEFb transcription elongation factor. *Proc. Natl. Acad. Sci. U.S.A.* 111: 7468–7473.

Woelfle, M.A., Ouyang, Y., Phanvijhitsiri, K. and Johnson, C.H. (2004) The adaptive value of circadian clocks: an experimental assessment in cyanobacteria. *Curr. Biol.* 14: 1481–1486.

Xie, K., Minkenberg, B. and Yang, Y. (2015) Boosting CRISPR/Cas9 multiplex editing capability with the endogenous tRNA-processing system. *Proc. Natl. Acad. Sci. U.S.A.* 112: 3570–3575.

Xie, Q., Wang, P., Liu, X., Yuan, L., Wang, L., Zhang, C., et al. (2014) LNK1 and LNK2 are transcriptional coactivators in the Arabidopsis circadian oscillator. *Plant Cell* 26: 2843–2857.

Yerushalmi, S., Yakir, E. and Green, R.M. (2011) Circadian clocks and adaptation in Arabidopsis. *Mol. Ecol.* 20: 1155–1165.

Zhang, C., Brown, M.Q., van de Ven, W., Zhang, Z.M., Wu, B., Young, M.C., et al. (2016) Endosidin2 targets conserved exocyst complex subunit EXO70 to inhibit exocytosis. *Proc. Natl. Acad. Sci. U.S.A.* 113: E41–E50.

Zhu, J., Liu, M., Liu, X. and Dong, Z. (2018) RNA polymerase II activity revealed by GRO-seq and pNET-seq in Arabidopsis. *Nat. Plants* 4: 1112–1123.

Zuckerkandl, E. and Pauling, L. (1965) Evolutionary divergence and convergence in proteins. In Edited by Bryson, V. and Vogel, H.J. Evolving Genes and Proteins. pp. 97–166. Academic Press, New York.